VICARIOUS CALIBRATION OF TERRA ASTER, MISR, AND MODIS

K. Thome, S. Biggar, H. J. Choi
Remote Sensing Group, Optical Sciences Center, University of Arizona, Tucson AZ 85721

ABSTRACT

The Advanced Spaceborne Thermal Emission and Reflection and Radiometer (ASTER), Multi-angle Imaging Spectroradiometer (MISR) and Moderate Resolution Imaging Spectroradiometer (MODIS) are all onboard the Terra platform. An important aspect of the use of MODIS, and other Earth Science Enterprise sensors, has been the characterization and calibration of the sensors and validation of their data products. The Remote Sensing Group at the University of Arizona has been active in this area through the use of ground-based test sites. This paper presents the results from the reflectance-base approach using the Railroad Valley Playa test site in Nevada for ASTER, MISR, and MODIS and thus effectively a cross-calibration between all three sensors. The key to the approach is the measurement of surface reflectance over a 1-km^2 area of the playa and results from this method shows agreement with MODIS to better than 5%. The paper examines biases between ASTER and the other two sensors in the VNIR due to uncertainties in the onboard calibrator for ASTER and in the SWIR due to an optical crosstalk effect.

Keywords: Absolute-radiometric calibration, vicarious calibration, atmospheric correction

1. INTRODUCTION

The Terra platform was launched in December 1999. The platform consists of a total of five sensors as part of NASAís Earth Science Enterprise. The three sensors used in this work are imaging sensors of varying spatial resolution, swath width, and view geometries. These sensors are the Advanced Spaceborne Thermal Emission and Reflection Radiometer (ASTER),[1] the Multiangle Imaging SpectroRadiometer (MISR),[2] and the MODerater Resolution Imaging Spectroradiometer (MODIS).[3]

ASTER is colloquially referred to as the zoom lens of the Terra platform. It has a 60-km swath width with 14 total bands in the visible and near infrared (VNIR), shortwave infrared (SWIR), and thermal infrared (TIR). The spatial resolution of the three VNIR bands is 15 m, that of the six SWIR bands is 30 m, and the five TIR bands have 90-m spatial resolution. The sensor also includes a backward pointing VNIR band that is used for stereo imaging to produce digital elevation models. The VNIR and SWIR sensors are pushbroom systems while the TIR uses a scan mirror approach for crosstrack coverage.

MISR has moderate swath width and resolution with the capability to collect data at 250-m spatial resolution at nadir and a 360-km swath. It has four spectral bands in the VNIR using a pushbroom approach. The defining characteristic of MISR is that it has nine separate cameras pointed at a variety of angles. These multiple views provide directional scattering information from the surface and atmosphere allowing retrievals of atmospheric aerosols and surface bi-directional reflectance. Only the nadir-viewing camera is considered in this work.

The third sensor on the Terra platform that is included here is MODIS. MODIS is a scanning system bordering on being a hyperspectral sensor in that it has 36 spectral bands. It too has varying spatial resolution with two land bands having 250-m resolution, five land bands at 500-m resolution, and the rest of the bands with 1-km resolution. The lower spatial resolution and scanning design allows MODIS to have a wide swath that gives global coverage every two days. There are two separate MODIS instruments currently in orbit, one on the Terra platform with a descending morning crossing time and Aqua with an afternoon crossing time in ascending mode, though only Terra MODIS is considered here.

Earth Observing Systems IX, edited by William L. Barnes, James J. Butler, Proc. of SPIE
Vol. 5542 (SPIE, Bellingham, WA, 2004) · 0277-786X/04/$15 · doi: 10.1117/12.559942

One of the primary efforts for the use of MODIS data is to develop synergy between the morning and afternoon data sets to improve understanding of land, ocean, and atmospheric processes. This synergistic approach to the data is also one of the purposes of the multi-sensor Terra platform. The goal is that combinations of data from the multiple sensors provides more insight than each of the individual sensors alone. This synergy clearly requires that data from the sensors are consistent from a radiometric standpoint. That is, two sensors should report the same band-averaged spectral radiance when subject to the same input spectral radiance. Such consistency necessitates an accurate radiometric calibration of the sensors.[4]

The EOS program has taken great care during the preflight phase of the sensor characterization to ensure accurate calibration of each of the individual sensors. In addition, efforts were made to ensure the consistency of these laboratory calibrations across the multiple national standards and individual vendor calibration facilities.[5,6,7,8] It was also expected that the Terra sensors would degrade once in orbit. Thus, each of the sensors, including ASTER, MISR, and MODIS make use of onboard calibrators to maintain an accurate retrieval of at-sensor spectral radiance throughout the mission lifetime. ASTER relies on a set of incandescent lamps as calibration sources in the VNIR.[6] MISR and MODIS monitor sensor degradation through the use of solar diffusers.[9,10] The degradation of the diffusers is monitored in both cases with MISR relying on a photodiode monitor and MODIS using a ratioing radiometer.[9,11]

Unfortunately, it is still possible that biases can exist between the sensors or that the onboard calibration could fail or not operate properly. Thus, vicarious approaches are employed as a further check on the sensorís radiometric behavior. The Remote Sensing Group (RSG) at the University of Arizona has exploited these vicarious methods to calibrate both low- and high-spatial-resolution sensors with accuracies in the 2-5% range.[12,13,14,15,16,17,18]

This work extends the reflectance-based approach to the MISR sensor. Then, by using the reflectance-based approach as a reference calibration, it becomes possible to compare the results from ASTER, MISR, and MODIS to determine if any significant biases occur between these sensors. The next section briefly summarizes the reflectance-based approach and the Railroad Valley test site used for this work. This is followed by results for MISR from a set of 11 dates for which ground-based measurements were collected for the MODIS sensor. The MISR results are then compared with those of the ASTER and MODIS sensors where the ASTER results included data from all sites as well those from only the Railroad Valley Playa. These comparisons show that MODIS and MISR agree with each other to better than 3% for the four bands of MISR while early ASTER data differ by as much as 20% and newer data by as much as 5%. Large differences also exist between ASTER and MODIS in the shortwave infrared due to the optical crosstalk effect in ASTER. In addition, results from July 16, 2001 are presented from MODIS and MISR as this date has been used in the past as a comparison between six sensors and the inclusion of MISR brings that number to seven.

2. METHODOLOGY

The reflectance-based approach and Railroad Valley Playa have been described in detail in previous work. A brief summary is given here for completeness, but the reader is directed elsewhere for more information.[12,13,17] The test site used in this work is the Railroad Valley Playa that is on Bureau of Land Management land in central Nevada. The overall size of the playa, approximately 15 km by 15 km, makes it suitable for the larger footprints of MODIS and MISR. The playaís 1.5 km elevation, its location in a region with typically clear weather and low aerosol loading, and its high surface reflectance makes it a good site for the reflectance-based approach. Typical atmospheric conditions at the site include an aerosol optical depth at 550 nm that is less than 0.05 and horizontal visibilities in excess of 60 km. Peak precipitation occurs in winter between December and March and also during the summer months of July and August. The reflectance of the playa is generally greater than 0.3 and relatively flat spectrally except for the blue portion of the spectrum and an absorption feature in the shortwave infrared. Ground-based measurements of the directional reflectance characteristics of the playa show it to be nearly lambertian out to view angles of 30 degrees for incident solar zenith angles seen for overpasses of Terra.[19]

The reflectance-based method uses measurements to characterize the surface of a test site and the atmosphere over that test site. The results of these characterizations are inputs to a radiative transfer code to predict at-sensor radiance. The

approach was first applied in 1984 to Landsat-5 Thematic Mapper.[12,13] The surface reflectance retrieval relies on transporting a spectroradiometer across a selected area. The approach adopted for large footprint sensors is to cover a 1-km by 1-km area with eight 500-m paths in a cross-like pattern. This approach has the advantage of characterizing some of the broad scale changes in the site in orthogonal directions. The site used for smaller footprint sensors is much smaller with the goal to collect 8-10 samples within a linear path through a given spatial pixel. A total of 30 to 64 pixels are sampled depending on the sensor. The other primary input to the radiative transfer code is the atmospheric conditions at the time of sensor overpass and these are obtained from solar extinction measurements.

The same basic method is applied to all three sensors in this work. The atmospheric conditions on a given date for a given sensor are identical for all three sensors since all three are on the same platform. Likewise, the view-sun geometry is identical for all three. Thus, the only differences between the sensors are the spectral reflectance data and the spectral bands themselves. The spectral effects are taken into account by computing the at-sensor radiance via a radiative transfer code at 1-nm intervals from 350-2500 nm. These hyperspectral, predicted radiances are band-averaged using the appropriate spectral response of a given band to determine the in-band spectral radiance.

Table 1 lists the bands that are discussed in this work. The wavelengths given are center wavelengths based on a band-averaging approach and they are listed according to each sensorís numbering convention. The five TIR bands for ASTER are ignored here as is the backward looking VNIR band (band 3B). The fact that the MODIS bands are not ordered from short to long wavelength is the outcome of the fact that MODIS bands are labeled according to application and resolution. Bands 1 and 2 are 250-m resolution bands for land studies. Bands 3-7 are the 500-m bands also used primarily for land studies. Band 8 is a 1-km ocean band and thus has very high radiometric sensitivity, however, Railroad Valley Playa is dark enough that this band does not saturate over the playa. Thus, band 9 is omitted due to saturation effects, as are bands 10-16. All other bands, except band 17, are either thermal infrared bands or are significantly affected by atmospheric absorption. The intercomparison results shown in this work focus on the VNIR bands that are common to the three sensors. Results for the SWIR are also given, but these obviously focus on the ASTER and MODIS sensors.

The predicted radiance based on the vicarious results are compared to the reported radiance from the three sensors to determine differences between the reported and predicted radiance. All of the results shown here rely on Level-1B data for ASTER and MODIS obtained from NASAís EOS Data Gateway. These data correspond to radiometrically-, but not geometrically-corrected data. MODIS data were omitted in all instances when a faulty detector was present over the region of interest. Conversion of the Level-1B digital counts was accomplished using the conversion factor supplied in each individual data setís EOS Hierarchical Data Format (HDF) file. The MISR data used in this work was obtained directly from the Langley DAAC. These data are Level L1B2 terrain data resampled and topographically corrected. Typically, the RSG uses data that have not been resampled, but the uniformity of the test site should limit the effects of the resampling, while the benefit of having geometrically corrected data greatly simplifies the location of the test site in the imagery. Conversion to radiance is accomplished via scale factors supplied with the data.

Table 1. Nominal center wavelengths of ASTER, MISR, and MODIS are given here as determined by band-averaging relative to the solar spectrum.

Band	ASTER	MISR	MODIS
1	0.554	0.445	0.645
2	0.661	0.558	0.856
3	0.807	0.672	0.466
4	1.652	0.867	0.553
5	2.164	N/A	1.243
6	2.204	N/A	1.632
7	2.259	N/A	2.119
8	2.329	N/A	0.412
9	2.394	N/A	Saturated
17	N/A	N/A	0.904

3. MISR REFLECTANCE-BASED RESULTS

The above approach has been applied to 11 dates from MISR. Figure 1 shows the percent difference between the predicted reflectance-based results and the reported MISR radiances for each of the 11

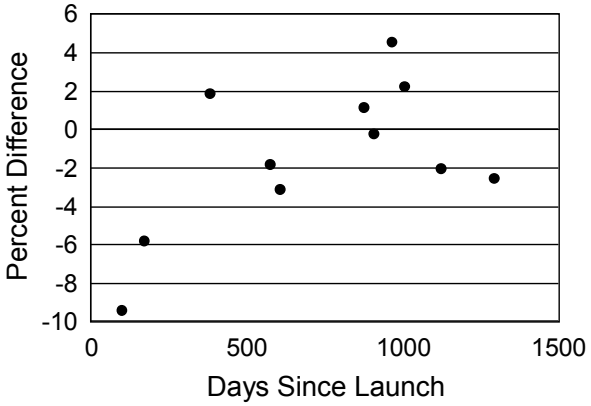

Figure 1. Percent difference computed between the predicted and reported at-sensor radiance for MISR band 2 (558 nm) from data collected at Railroad Valley Playa.

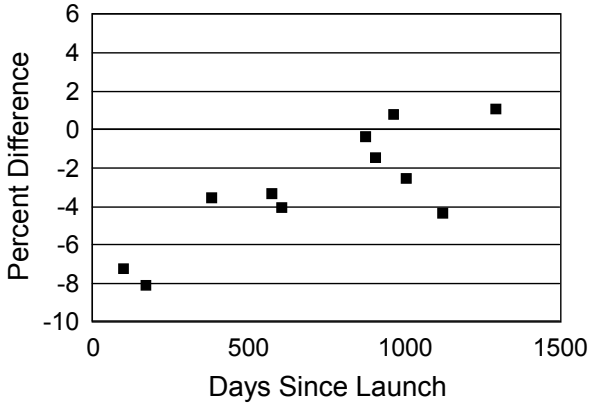

Figure 2. Percent difference computed between the predicted and reported at-sensor radiance for MODIS band 4 (553 nm) from data collected at Railroad Valley Playa for the same dates as shown in Figure 1.

dates for Band 2. The results for the other bands are similar and indicate that there is no strong temporal effect in these data except for the first two data points. These data points are most likely inherent to the ground data as can be seen in Figure 2 which shows the MODIS results for the same dates as those shown in Figure 1. Thus, it can be seen that both MISR and MODIS show similar behavior on these two early dates indicating that a portion of the percent difference is inherent to the reflectance-based measurements.

It should be pointed out that the first data point shown in the figures for both sensors is from a date with an eight-degree view angle. Thus, a portion of the larger difference could be an uncorrected effect in the directional nature of the surface reflectance. In addition, there could be instrumental effects in both sensors that manifest themselves at larger view angles. This, however, would be an unlikely coincidence. One coincidence that is possible, and could explain the larger differences in both sensors, is that these points represent data sets from very early in the mission lifetime of the Terra platform. Processing methods and knowledge of the sensorsí behavior have improved since these early data sets and reexamining the image data could lead to improved results.

In other cases, the results between MODIS and MISR do not follow one another. A good example of this is seen in the third data point for both sensors (383 days after launch). This point shows good agreement with the next two data sets for MODIS but not MISR. This could be an instrumental effect in MISR, or it could be a registration difference between MODIS and MISR. This misregistration effect is applicable even though MODIS and MISR are viewing at the same angle at the same time. The MODIS band shown in Figure 2 is from a 500-m spatial resolution sensor while that of MISR is 250 m. Thus, it is possible that the area of the ground measured by the ground-based instrumentation may not correlate well to the imagery data for one or both of the sensors. Thus, a portion of the different behavior between the two sensors is most likely due to the difficult nature of matching the geographic location of the ground data to the actual image data.

Averaging all of the data points shown in Figure 1 (excluding the first two points), gives the results shown in Figure 3. This figure summarizes the results for all bands of MISR and gives the average percent difference between the reported and predicted radiance. The average is that computed from the nine dates and the size of the bars for each band corresponds to the standard deviation of this average. The results in Figure 3 indicate that there is good agreement between the RSG results and the reported values from MISR. Bands 1 and 2 agree to within 1% of the RSG reflectance-based measurements and bands 3 and 4 to within 3%. The size of the error bars shown in Figure 3 are an indication of the precision of the vicarious results and this is better than 3% in all bands.

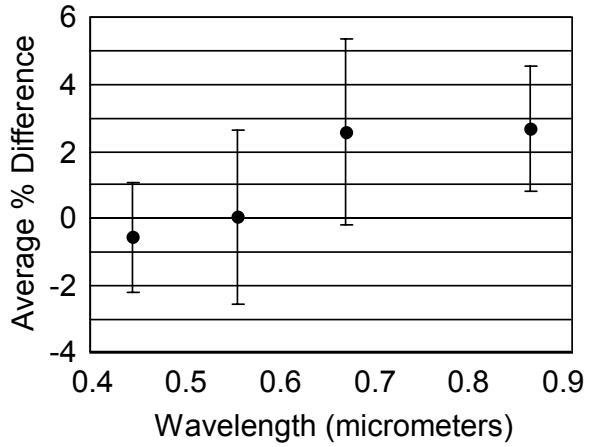

Figure 3. Average percent difference between MISR image-based results and predicted values from reflectance-based measurements

Care must be taken in evaluating Figure 3 because there is a strong traceability to the RSG results in the MISR calibration approach.[20,21] Issues with the behavior of the MISR onboard calibrator caused the MISR team to rely heavily on vicarious calibration results in developing their calibration. This was done using data from Railroad Valley from ETM+, the RSG, and an airborne simulator of MISR. Thus, one would expect there to be good agreement as shown in Figure 3. The results are still encouraging in that the precision of the results are very similar to that seen with other sensors using the same Railroad Valley test site.

4. ASTER, MISR, MODIS COMPARISONS

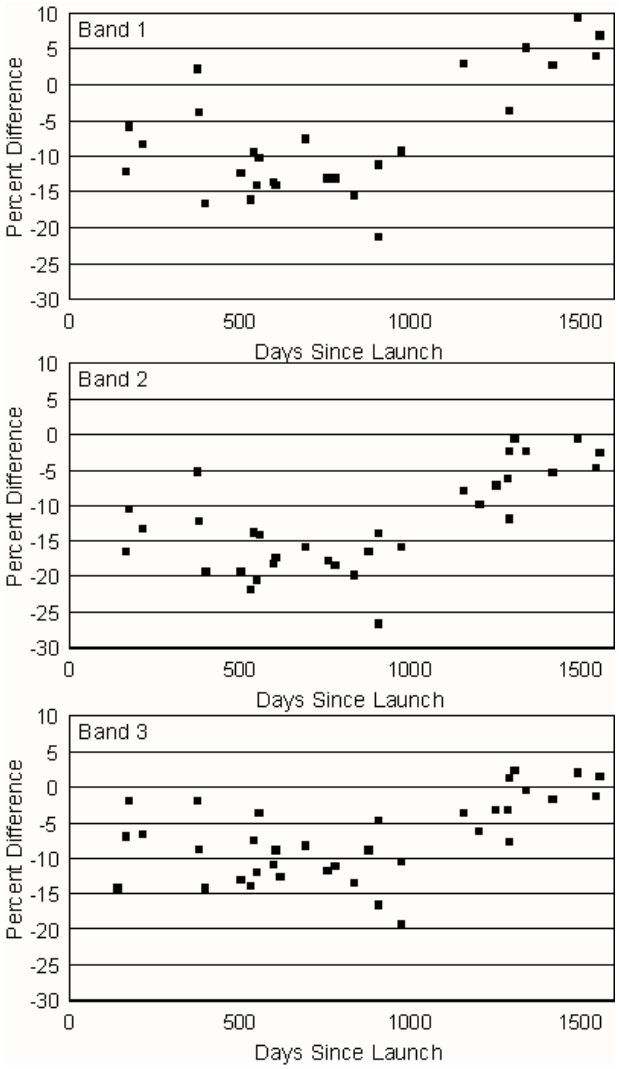

Figure 4. ASTER reflectance-based results from VNIR bands (1-3).

Figure 4 summarizes the results to date for ASTER for all test sites used by the RSG. Only bands 1-3 are shown since these correspond to the spectral region covered by MISR. The results shown in the figure are the percent differences between the vicarious predictions and the reported radiance as a function of date for all of the bands of interest. Negative values in this figure indicate that the predicted at-sensor radiance is larger than that reported by the sensor. The results in this figure indicate that all bands appear to have temporal effects. It should be recalled that the results shown here are based on the Level 1B radiance output from the sensor. This Level 1B product should include effects due to sensor degradation, thus any indication of temporal effects indicates that the Level 1B product is not taking into account the degradation effects.

The temporal effect appears to be largest for band 1. Analysis of the early ASTER data indicates that degradation of the ASTER data as seen in the Level 1A data is largest for Band 1 and this degradation slows considerably by day 1000. The abrupt change seen in the percent difference results of Figure 3 for Band 1 around day 1000 is due to a change in the radiometric calibration coefficients used in the processing stream. These two effects are also present in bands 2 and 3, though to a lesser extent. The ASTER VNIR bands are the only bands from the three Terra sensors studied in this work that shows a significant temporal trend in the Level 1B data product.

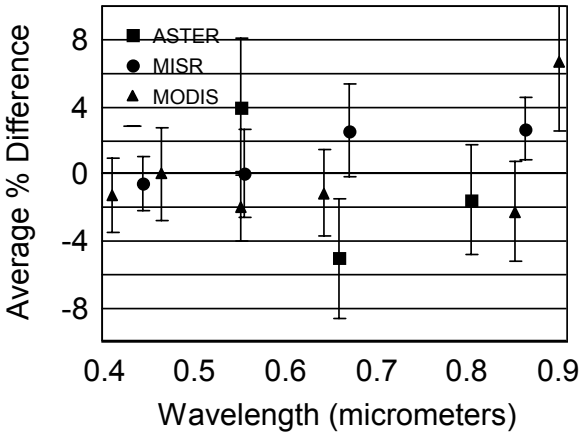

Figure 5. Average percent difference between predicted and reported radiance for ASTER, MISR and MODIS on Terra platform.

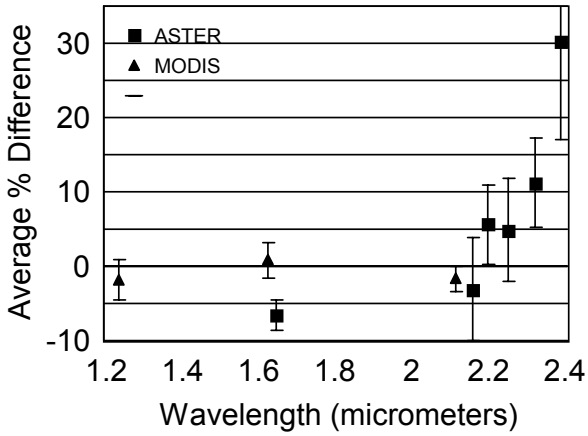

Figure 6. Average percent difference between predicted and reported radiance for ASTER and MODIS on Terra platform

Figures 5 and 6 are similar graphs to that shown in Figure 3 except now the results from each of the three sensors is given. Figure 5 shows the VNIR bands of each sensor and the MISR results shown are identical to those in Figure 3. The MODIS results are from the same dates as MISR and are thus directly comparable. The ASTER results are from only those data sets from after the recent change in calibration coefficients for the VNIR bands and also after the early lifetime degradation. This leads to the use of 12 dates of data, though one date had only VNIR bands, and five dates were saturated for band 1. It is also important to note that half of the dates are from the Railroad Valley Playa while the others are from the smaller Ivanpah Playa. Excluding the Ivanpah data sets does not impact strongly the results but gives a data set that is more statistically similar for comparison to the other sensors. In addition, the data from Railroad Valley Playa for ASTER are from measurements of a smaller test site that is approximately 700 m north of the site measured for MODIS and MISR.

The results of note seen in Figure 5 are that there is good agreement between the three sensors in the VNIR and the all sensors show similar standard deviations of the average with MISR showing the smallest standard deviations and ASTER the largest. MISR and MODIS agree to better than 4% in all bands and better than 2% in equivalent MISR bands 1and 2. It should be noted that the larger difference in band 4 appears to be consistent with the behavior of MODIS bands 2 and 17. It should be further noted that the band 17 behavior of Terra MODIS is also seen in Hyperion on the Earth Observer-1 platform and the MODIS sensor on Aqua. The agreement between ASTER and the other two sensors is also reasonably good for the more recent data sets. ASTER band 1 shows a difference of more than 6% with MODIS band 4 and ASTER band 2 has a 7% difference with MISR band 3. This is a significant difference when considering the expected accuracy of the vicarious results is 3% and the precision is better than this.

Of greater concern are the results seen in the shortwave infrared shown in Figure 6. Band 4 of ASTER and Band 6 of MODIS disagree by more than 6%. While this is within the accuracy of the vicarious calibration, the precision of the method indicates that these two bands have significantly different radiometric response. The other spectral bands of ASTER show large standard deviations and the percent differences for bands 6-9 are much larger than those seen for MODIS. The cause of both effects is due to a known optical crosstalk effect in ASTER. This phenomenon causes light from band 4 to be scattered into the other bands.

The optical crosstalk effect seen in the SWIR bands is a dominant issue for the large, bright vicarious calibration sites. This effect is most dominant in band 9 due to the proximity of the detectors of band 9 to the band 4 detectors. In addition, the longer wavelength of band 9 relative to band 4 leads to much lower spectral radiances in band 9 due to the

lower incident solar spectral irradiance. Water vapor absorption effects in band 9 further reduce the in-band radiance relative to the scattered radiance from band 4. Thus, the ASTER results are difficult to interpret in the SWIR and work is underway to apply a cross-talk correction to determine if this improves the radiometric quality of the data.[22]

5. JULY 16, 2001 INTERCOMPARISON

The results from the previous section show how well the primary imaging sensors on the Terra platform compare with each other. In addition, there is a desire to understand how well these sensors compare with other imaging sensors that are part of NASAís Earth Science Enterprise. One date, 2001-07-16, provided an opportunity for the intercomparison of a large number of sensors at the Railroad Valley Playa. Results from this date have been previously presented for ALI, Hyperion, Ikonos, ETM+, MODIS, and SeaWiFS.[23, 24] Unfortunately there were issues with the ASTER sensor on this date, and there are no image data from ASTER on this date. This work now adds the MISR data as well.

Figures 7 and 8 show the results from a cross-calibration approach to the processing of ground data from July 16, 2001. This approach has been described previously and is only briefly repeated here.[22,23] Essentially, the cross-calibration approach uses image data from ETM+ for a selected area of Railroad Valley Playa to derive a hyperspectral surface reflectance for a large region of the playa. The ETM+ data are converted to spectral radiance using the preflight radiometric calibration coefficients and then atmospherically corrected using results from ground-based measurements of solar transmittance. The ETM+ multispectral surface reflectance results are used to scale ground-based hyperspectral reflectance data to obtain a predicted hyperspectral surface reflectance for the playa.

The predicted hyperspectral surface reflectance is assumed to be lambertian and invariant with time. It is used in a radiative transfer code along with the geometry of the desired sensor, atmospheric conditions for that sensor, and the solar zenith and azimuth to predict an at-sensor, hyperspectral radiance. The at-sensor radiance is determined using the specific spectral solar irradiance curve for each sensor.[25] Finally, the hyperspectral radiance is band-averaged for the spectral bands of each sensor to give a predicted, in-band, at-sensor spectral radiance.

It should be pointed out that all of the results shown in this section rely on the most recent understanding of the radiometric calibration of each sensor. For MODIS, this implies that a recent Level 1B data set was received from the EOS Core System and calibration information provided in the metadata was used. The coefficients used to correct the Ikonos data are those supplied by Space Imaging for data sets provided after February 2001. ALI and Hyperion results depend upon calibration coefficients derived in December 2001. These coefficients included large corrections for bands 1p and 5 of ALI and approximately a 10% correction for Hyperion. The corrections for the EO-1 sensors were based on information from lunar views, the onboard solar diffusers, and vicarious calibrations using the reflectance-based approach.

The results in Figure 7 show only the VNIR bands from MODIS, MISR, and ETM+ to allow a clearer comparison of these sensors. Recall that ETM+ was used to determine the surface reflectance model for the cross-comparison. Thus, a perfect surface model application would have given no difference between ETM+ image-based radiances and those predicted from the cross-comparison approach. Then, differences seen in Figure 7 for ETM+ are an indication of the error in the spectral nature of the surface model. This error does not impact the relative

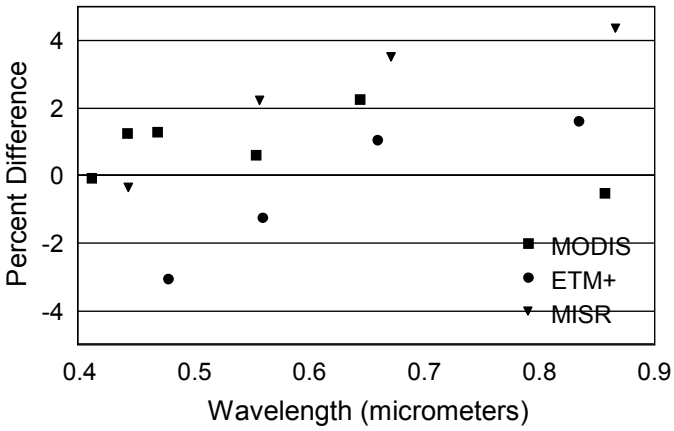

Figure 7. Cross-comparison results for MODIS, MISR, and ETM+ from July 16, 2001 data at Railroad Valley Playa. Only VNIR bands for all threes sensors are shown. No ASTER data are available from this date.

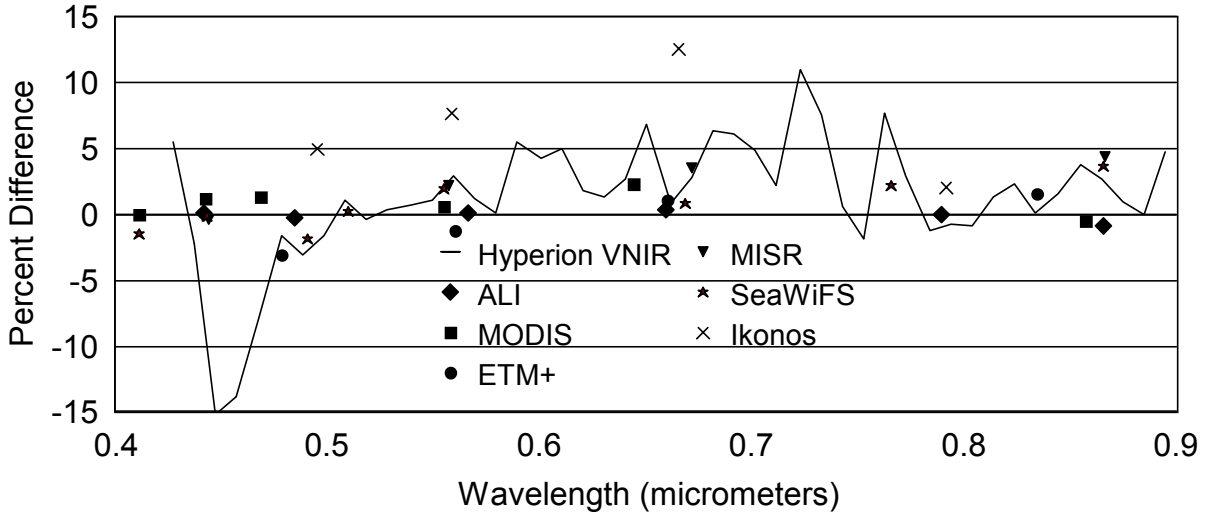

Figure 8. Results of cross-comparison study from July 16, 2001 at Railroad Valley using ETM+ as a reference

comparisons between sensors except that for small band-to-band effects due to errors in the spectral shape of the surface reflectance. The results shown in Figure 7 agree well with those of Figure 5 (note the additional MODIS band in Figure 7 related to an unsaturated band 9). That is, the best agreement is at shorter wavelengths with bands 1 and 2 agreeing between the two sensors to better than 2% and band 4 showing the largest disagreement with a value near 4%. The agreement between ETM+ and MISR follows an opposite trend with the difference being largest in band 1 (approximately 4%) and smallest in band 4 (approximately 3%).

The results from all of the seven sensors is shown in Figure 8. These results indicate that, with the exception of a few Hyperion bands and bands 2 and 3 of Ikonos, all of the sensors shown agree to better than +/- 3%. This is rather remarkable considering the range of spatial resolutions, overpass times, view angles, sensor ages. It is also a testament to the efforts of the groups performing the preflight and inflight characterizations of these sensors. It should be noted that the only sensors in Figure 8 in which no data from the RSG have been used to assist in determining the inflight radiometric calibration are ETM+, MODIS and SeaWiFS. All of the other sensors have included RSG reflectance-based results in the data sets used to adjust the inflight radiometric calibration. ETM+, MODIS, and SeaWiFS have relied on RSG data (both preflight and inflight) to assist in evaluating the status of the radiometric calibration.

6. CONCLUSIONS

Previous work related to MODIS data only concluded that the reflectance-based approach can be applied accurately to large-footprint sensors. This work also concluded that consistent application of this approach to multiple sensors allows for a cross-calibration of these sensors relative to the vicarious results. It is this concept that has been applied here to ASTER, MISR, and MODIS. Comparison of the biases between these three sensors to the reflectance-based results allows biases between the three sensors relative to the vicarious results to be found.

These relative comparisons show that the recent change in the radiometric calibration coefficients for ASTER have greatly improved the radiometric compatibility of the VNIR bands to other sensors. There are still larger than desired differences between ASTER, MISR, and MODIS in band 1 of ASTER and it is recommended that users take this difference into account when using all three sensors to examine scalability issues. MODIS and MISR show better agreement in the VNIR than with ASTER and this difference is smaller than the combined radiometric uncertainty of the sensors. It is possible, however, to improve the agreement between the two sensors by forcing them to both fit a similar radiometric scale. This work does not recommend a specific scale, and further data sets are needed to determine

the repeatability of the results shown here, but the average differences seen here are a first step in creating a radiometrically consistent data set.

The cross-comparison work via the reflectance-based results has also been verified via a separate cross-comparison approach using data from Landsat-7 ETM+ along with four other sensors in addition to MODIS and MISR. This approach showed that the five sensors (ALI, ETM+, MISR, MODIS, and SeaWiFS) agreed to better than 5% (+/- 2.5%) in all VNIR bands. Hyperion and Ikonos also showed good agreement in all but a few bands.

The overall conclusions of this work are that vicarious methods are proving to be an excellent approach for cross-comparing the radiometric response of remote sensing systems and the use of a well-understood test site such as Railroad Valley Playa is helpful in applying these vicarious approaches. Such results will have ever increasing importance as the possibility of data gaps in such data sets as the Landsat-series of data increases. Vicarious methods can now provide a method for closing these possible data gaps allowing for the long-term records to be extended even without overlap.

ACKNOWLEDGMENTS

We wish to acknowledge the Bureau of Land Managementís Tonopah office for the assistance in gaining access to the Railroad Valley Playa site. We would also like to acknowledge the efforts of the numerous individuals who assisted in collecting the ground-based data used in this work. This research was supported by NASA contract NAS5-31717 and NASA grants NAG5-1139 and NAG5-2448.

REFERENCES

1. Y. Yamaguchi, A. Kahle, H. Tsu, T. Kawakami, and M. Pniel, "Overview of Advanced Spaceborne Thermal Emission and Reflection Radiometer (ASTER)," *IEEE Trans. On Geoscience and Remote Sensing*, Vol. 36, 1998.
2. D.J. Diner, J.C. Berkert, T.H. Reilly, C.J. Bruegge, J.E. Conel, R.A. Kahn, J.V.Martonchik, T.P. Ackerman, R. Davies, "MISR Instrument Description and Experiment Overview", *IEEE Trans. On Geoscience and Remote Sensing*, Vol. 36, pp. 1072-1087, 1998
3. W. L. Barnes, T. S. Pagano, and V. V. Salomonson, "Prelaunch characteristics of the Moderate Resolution Imaging Spectroradiometer (MODIS) on EOS-AM1," *IEEE Trans. On Geoscience and Remote Sensing*, Vol. 36, pp. 1088-1100, 1998.
4. J. J. Butler and R. A. Barnes, "Calibration strategy for the Earth Observing System (EOS)-AM1 platform," *IEEE Trans. On Geoscience and Remote Sensing*, Vol. 36, pp. 1056-1061, 1998.
5. A. Ono, F. Sakuma, K. Arai, Y. Yamaguchi, H. Fujisada, P. N. Slater, K. J. Thome, F. D. Palluconi, and H.H. Kieffer, "Preflight and In-flight calibration plan for ASTER," *J. of Atmos. and Oceanic Tech*., Vol. 13, pp. 322-335, 1996.
6. C. J. Bruegge, V. G. Duval, N. L. Chrien, R. P. Korechoff, B. J. Gaitley, E. B. Hochberg, "MISR prelaunch instrument calibration and characterization results," IEEE Trans. On Geoscience and Remote Sensing, Vol. 36, pp. 1186-1198, 1998.
7. Butler, J. J., S. W. Brown, ..., "Radiometric measurement comparison on the integrating sphere source used to calibrate the Moderate Resolution Imaging Spectroradiometer (MODIS) and the Landsat-7 Enhanced Thematic Mapper Plus," *J. of Res. Of the Natíl Inst. of Standards and Technology*, 108, pp. 199-228, 2003.
8. Butler, J. J., B. C. Johnson, and R. A. Barnes, "Radiometric measurement comparisons at NASAís Goddard Space Flight Center: Part 1. The GSFC sphere sources," *The Earth Observer*, 14, pp. 3-7, 2002.
9. C.J. Bruegge, B.G. Chafin, N.C.L. Chrien, D.J.Diner, R. Ando, "In-flight calibration of the EOS/ Multi-angle Imaging SpectroRadiometer (MISR)", *Sensors, Systems, and Next Generation Satellites,* Vol. 4169-08, 2000.
10. X. Xiong, J-Q Sun, J. A. Esposito, B. Guenther, W. L. Barnes, "MODIS reflective solar bands calibration algorithm and on-orbit performance," *Proc. SPIE 4891*, pp. 95-104, 2003.
11. P.N. Slater and J.M. Palmer, "Solar diffuser and ratioing radiometer approach to satellite sensor onboard calibration," *Proc. SPIE 1493*, 1991.

12. P. N. Slater, S. F. Biggar, R. G. Holm, R. D. Jackson, Y. Mao, M. S. Moran, J. M. Palmer, and B. Yuan, "Reflectance- and radiance-based methods for the in-flight absolute calibration of multispectral sensors," *Rem. Sens. Env.*, Vol. 22, pp 11-37, 1987.
13. K. J. Thome, D. I. Gellman, R. J. Parada, S. F. Biggar, P. N. Slater, and M. S. Moran, "In-flight radiometric calibration of Landsat-5 Thematic Mapper from 1984 to present," *Proc. of SPIE*, Vol. 1938, 1993.
14. S. F., Biggar, P. N. Slater, and D. I. Gellman, "Uncertainties in the in-flight calibration of sensors with reference to measured ground sites in the 0.4 to 1.1 μm range," *Rem. Sens. Env.*, Vol. 48, pp. 242-252, 1994.
15. P. N. Slater, S. F. Biggar, J. M. Palmer, and K. J. Thome, "Unified approach to pre- and in-flight satellite sensor absolute radiometric calibration," *Proceedings of SPIE* , Vol. 2583, pp. 130-141, 1995.
16. P. M. Teillet, P. N. Slater, T. Ding, R. P. Santer, R. D. Jackson, and M. S. Moran, "Three Methods for the Absolute Calibration of the NOAA AVHRR Sensors In-Flight," *Rem. Sens. Env*., **31**, pp. 105-120, 1990.
17. K. Thome, N. Smith, K. Scott, "Vicarious calibration of MODIS using Railroad Valley Playa," *International Geoscience and Remote Sensing Symposium*, Syndey, Australia, 2001
18. K. Thome, E. Whittington, and N. Smith, "Radiometric calibration of MODIS with reference to Landsat-7 ETM+," *Proc. SPIE Conf. #4483*, San Diego, Calif., 2001.
19. P. Nandy, K. Thome, and S. Biggar, "Characterization and field use of a CCD camera system for retrieval of bi-directional reflectance distribution function," *Journal of Geophysical Research*, 106, pp. 11,957-11,966, 2001.
20. Carol J. Bruegge, Nadine L.Chrien, Robert R. Ando, David J. Diner, Wedad A. Abdou, Mark C. Helmlinger, Stuart H. Pilorz, Kurtis J. Thome, "Early Validation of the Multi-angle Imaging SpectroRadiometer (MISR) Radiometric Scale", *IEEE Trans, Geosci. Remote Sensing*, vol. 40, NO.7, July 2002
21. Wedad A. Abdou, James E. Conel, Stuart h. Pilorz, Mark C. Helmlinger, Carol J. Bruegge, Barbara J. Gaitley, William C. Ledeboer, John V. Martonchik, "Vicarious calibration: A reflectance-based experiment with AirMISR", *Remote Sensing of Environment,* Vol. 77, pp.338-353, 2001.
22. H. Tonooka and A. Iwasaki, "Improvement of ASTER/SWIR crosstalk correction," *Proc. SPIE #5234*, pp. 168-179, 2004.
23. K. J. Thome, S. F. Biggar, W. T. Wisniewski, "Cross-comparison of EO-1 sensors and other Earth Resources Sensors to Landsat-7 ETM+ Using Railroad Valley Playa," *IEEE Trans. On Geosciences and Remote Sensing,* 41, pp. 1180-1188, 2003.
24. K. Thome, R. Barnes, G. Feldman, "Intercomparison of ETM+, MODIS, and SeaWiFS using a land test site," *Proc. SPIE Conf. #4881*, pp. 319-326, Crete, Greece, 2002.
25. K . Thome,S. Biggar, and P. Slater, "Effects of assumed solar spectral irradiance on intercomparisons of earth-observing sensors," Proc. SPIE Conf. #4540, Toulouse, France, pp. 260-269, 2001.